Three Dimensional Simulation of Supersonic Flow over Missiles of Different Shapes

Dr.Jalal M. Jalil
Electromechanical Engineering Department, University of Technology/ Baghdad
Email: jalalmjalil@yahoo.com
Dr.Hussain H. Al-Kayiem
Engineering College, University of Almustansria/Baghdad
Dr.Ahmed Kadhim Hussein
Engineering College, University of Babylon/ Babylon

Received on: 7 /4/ 2011 & Accepted on: 5 /1/ 2011

ABSTRACT

In this work, a three-dimensional primitive variable of supersonic flow over missiles was computed based on finite difference computational fluid dynamic methods. The problem was considered is to deal with external, inviscid, compressible supersonic- flow over three-dimensional missiles with and without canard. Euler equations were solved using time-marching MacCormack's explicit technique. The flow conditions are taken at sea level and Mach number was tested up to 4.0. To deal with complex shape of missiles the so-called "body fitted coordinate system" was considered and the algebraic and elliptic methods were used to generate grids over missiles. The number of iterations and the number of mesh points depending on Mach number. The result indicate, that for the same Mach number, the increasing of mesh points, lead to increase of the number of iterations.

Keywords: Missiles, Supersonic flow, CFD, Numerical methods, Gas Dynamics, Supersonic aerodynamics, Euler equation.

تمثيل ثلاثي الابعاد لمجرى فوق الصوتي لمقذوفات ذات اشكال مختلفة

المقدمة

في هذا البحث, حسب الجريان فوق الصوتي الثلاثي البعدعبر مقذوفات بطريقة الفروقات المحددة لديناميك الموائع الحسابي. لقد اعتبرت المسألة ذات جريان خارجي فوق صوتي لاأنضغاطي غيرلذج عبر مقذوفات ثلاثية البعد مع كنرد تقليدي وبدون كنرد. حلت معادلات أويلرباستخدام تكنيك مكورمك الظاهرمع الوقت. ظروف الجريان أخذت عند مستوى سطح البحر مع عدد ماخ لغاية 2.5 للتعامل مع الشكل المعقد للمقذوفات, استخدمت نظام احداثيات مطابقة الجسم بالطرق الجبرية والبيضوية لتوليد الشبكة عبر المقذوفات. اظهرت النتائج تطابق جيد مع النتائج المنشورة.

INTRODUCTION

Supersonic flow was a flow in which a Mach number is greater than 1.0, and this flow is very important in the design of aircraft and rockets. During the past, the experimental and analytical methods were used to simulate the properties of supersonic flow over a limited number of shapes, but for supersonic three-dimensional shapes such as a 3D supersonic missile, the analytical method did not satisfied due to non-linearity also to design an aircraft or missile many thousands of tests were drawn in a supersonic wind tunnel which requires a hard and expensive work and require a very long time. In contrast, a numerical prediction give the same result with a short-time and an accurate computation and the computer program may be changed easily to deal with any other sort of supersonic missile [1]. Morgenstern [2] simulated the unsteady, viscous, supersonic flow over a spike-nosed body of revolution numerically by solving Navier-Stokes equations. Scalabrin et al. [3] simulated the aerodynamic flow over a multi-stage rocket by using finite element method while Wilcox et al. [4] presented a wind tunnel investigation of a square cross-sectional missile configuration in order to obtain force and moment measurements. Blades and Marcum [5] demonstrated grid approach for the aerodynamic simulations of a spinning missile. Erickson [6] applied a pressure-sensitive paint technique in a wind tunnel experiment to quantify the vortex-induced surface static pressure on a slender missile. Wu et al. [7] presented the results of using arc-length mesh generation to predict the reducing in drag forces of grid fin and missile in a supersonic flow region. Cvitanovic et al. [8] applied the pannel method for the analysis of potential flow a round a wing-body configuration. DeSpirito et al. [9] used viscous computational fluid dynamic simulations to predict the aerodynamic coefficients and flow field around a canard-controlled missile in a supersonic flow.

In the present work, the complex differential equations are overcome by replacing it with differences, calculated from a finite number of values associated with the computational nodes, which are distributed on a suitable grid over the solution domain. The predictor-corrector MacCormack's explicit finite difference method was used to predict the aerodynamic properties of three-dimensional external compressible inviscid supersonic flow, such as pressure, Mach number and temperature at each grid. The time - marching method was chosen to treat a supersonic missile with conventional canard, long canard and with no canard. The shapes of the missiles which studied in the present work and their dimensions are shown in Figure 1.

MATHEMATICAL ANALYSIS

The supersonic flow in this study treats with a non-viscous, non-heat conducting fluid, so it is described by Euler equation. The latter is obtained from Navier-Stokes equations by neglecting all shear stresses and heat-conduction terms, so it is a valid approximation for flows at high speed (supersonic flow), i.e., at high Reynolds number outside the viscous region developing near the solid surface. The mathematical behavior of the Euler equation is classified as hyperbolic in supersonic flow **[10].** The solution is obtained using time-marching method. In this method three points must be noticed.

1. The grid points are generated in physical plane and transformed to computational plane before solving governing equations.
2. The solution is obtained by marching from some initial flow field with time until a steady – state is obtained.
3. The governing equation for an inviscid, non-heat conducting, external, compressible, three-dimensional supersonic flow expressed in conservation form are **[11]:**

Continuity equation:

$$\nabla.(\rho V)=\frac{\partial \rho}{\partial t}+\frac{\partial(\rho u)}{\partial x}+\frac{\partial(\rho u)}{\partial y}+\frac{\partial(rw)}{\partial z} \quad \ldots(1)$$

The conservation of momentum equation is :

$$\frac{\partial(\rho u)}{\partial t}+\frac{\partial(\rho u^2+p)}{\partial x}+\frac{\partial(\rho u u)}{\partial y}+\frac{\partial(ruw)}{\partial z}=0$$

$$\frac{\partial(\rho u)}{\partial t}+\frac{\partial(\rho u u)}{\partial x}+\frac{\partial(\rho u^2+p)}{\partial y}+\frac{\partial(rvw)}{\partial z}=0 \quad \ldots(2)$$

$$\frac{\partial(\rho w)}{\partial t}+\frac{\partial(\rho u w)}{\partial x}+\frac{\partial(rwv)}{\partial y}+\frac{\partial(rw^2+p)}{\partial z}=0$$

The conservation of energy equation is:

$$\frac{\partial(rE_t)}{\partial t}+\frac{\partial}{\partial x}[(rE_t+p)u]+\frac{\partial}{\partial y}[(rE_t+p)u]+\frac{\partial}{\partial z}[(rE_t+p)w]=0 \quad \ldots(3)$$

It is suitable to put these equations in a vector form before applying a numerical scheme to these equations. The 3-dimensinal Euler equation may be arranged in a vector form as:-

$$\frac{\partial Q}{\partial t}+\frac{\partial E}{\partial x}+\frac{\partial F}{\partial y}+\frac{\partial G}{\partial z}=0 \quad \ldots(4)$$

Where Q, E, F and G are column vectors which is defined by:

$$Q=\frac{\partial}{\partial t}=\begin{bmatrix} r \\ ru \\ rv \\ rE_t \end{bmatrix};E=\frac{\partial}{\partial x}=\begin{bmatrix} ru \\ ru^2+P \\ ruv \\ (rE_t+P)u \end{bmatrix};F=\frac{\partial}{\partial y}=\begin{bmatrix} rv \\ ruv \\ rv^2+P \\ (rE_t+P)v \end{bmatrix};$$

$$G=\frac{\partial}{\partial z}=\begin{bmatrix} rw \\ ruw \\ rw^2+P \\ (rE_t+P)w \end{bmatrix} \qquad \ldots(5)$$

Also the equation of state is given by:-

$$p = rRT$$

at ambient temperature, it becomes:-

$$r_\infty=\frac{p_\infty}{RT_\infty} \qquad \ldots(6)$$

And the free stream Mach number is given by:-

$$M_\infty = V_\infty / \sqrt{gRT_\infty}$$

The total pressure and temperature (or stagnation pressure and temperature) are given by: -

$$p_o=p_\infty\left[1+\frac{(g-1)}{2}M^2\right]^{\frac{g}{g-1}} \qquad \ldots(7)$$

$$T_o=T_\infty\left[1+\frac{(g-1)}{2}M^2\right] \qquad \ldots(8)$$

Moreover the velocity components are given by: -

$$u_\infty = V\cos a \qquad \ldots(9)$$

$$u_\infty = V\sin a \qquad \ldots(10)$$

Where $V = M\,a_\infty$ noting that:-

M = Mach number, and a_∞ = speed of sound

V =Fluid velocity

m_∞ = Free stream dynamic viscosity.

From the other hand, the following properties are detailed in Table 1

Table (1) Physical conditions of the current work

No.	*Altitude (m)*	P_∞ (Pa)	T_∞ (K)	r_∞ $\left(kg/m^3\right)$	V(m/sec)	M
1.	1500	84643.11	278.41	1.0593	501.6	1.5
2.	6000	49341.985	249.16	0.690	791.0	2.5
3.	14000	18903.83	197.16	0.33407	1055	3.75
4.	16000	14872.47	184.16	0.28138	1088.08	4.0

THREE- DIMENSIONAL MESH GENERATION

In this work, the algebraic grid generation method is used to produce mesh. This method generates grid points in space by means of interpolations based on given boundary data. Because of the non-uniform shape of missile, a body-fitted coordinate system is used which enable us for the transformation of governing equations from a Cartesian system **(x, y, z)** to a general curvilinear system **(**z ,h,x **)** and it help us to transform from physical plane to the computational plane **[10]**. The transformation of any partial differential equations from physical plane **(x, y, z)** to computational plane **(**z ,h,x **)** are defined by the following relations:

$$x = x\ (x, y, z) \qquad \ldots(11\text{-A})$$

$$z = z\ (x, y, z) \qquad \ldots(11\text{-B})$$

$$h = h\ (x, y, z) \qquad \ldots(11\text{-C})$$

The details of transformation are found in **[10]** and the results are given by:

$$J = \frac{1}{x_x\left[y_h z_z - z_h y_z\right] - x_h\left[y_x z_z - z_x y_z\right] + x_z\left[y_x z_h - z_x y_h\right]} \qquad \ldots(12)$$

Where, J is the Jacobian of transformation. It is defined as the ratio of the volumes in the physical space to that of the computational space. Also the metrics of transformation are given (in 3-D domain) as follows:-

$$\begin{aligned} x_x &= J\left[y_h z_z - y_z z_h\right] & h_x &= -J\left[y_x z_z - y_z z_x\right] \\ x_y &= -J\left[x_h z_z - x_z z_h\right] & h_y &= J\left[x_x z_z - x_z z_x\right] \\ x_z &= J\left[x_h y_z - x_z y_h\right] & h_z &= -J\left[x_x y_z - x_z y_x\right] \end{aligned} \qquad \ldots(13\text{-A})$$

And

$$z_x = J\left[y_x\ z_h - y_h\ z_x\right]$$
$$z_y = -J\left[x_x\ z_h - x_h\ z_x\right] \qquad \ldots(13\text{-B})$$
$$z_z = -J\left[x_x\ y_h - x_h\ y_x\right]$$

the physical meaning of the metrics is that, it represents the ratio of arc length in the computational space to that of the physical space. The terms x_z , x_h , y_z … are computed numerically using forward approximation, as an example **[12]**:-

$$y_h = \frac{\partial y}{\partial h} = \frac{-3y_{i,j,k} + 4y_{i,j+1,k} - y_{i,j+2,k}}{2\Delta h} \qquad \ldots(14)$$

NUMERICAL SCHEME

Explicit time-dependent solution of the three-dimensional Euler equations has been performed using MacCormack's predictor-corrector finite difference technique, which is second-order accurate in both space and time. This method is very effective finite difference technique for viscous and inviscid supersonic flow, especially for unsteady flow shock capturing. By using this technique a computer code is constructed to predict the shock wave which consists from the following steps:

1. A three-dimensional domain is chosen over a missile (21, 16, 21).
2. A grid generation is performed in (**x-y-z)** direction and the Jacobian and different metrics are calculated.
3. A flow conditions such as **(u, v, w, M, T, e,** r and **P)** are computed at the surface and then there are computed in the domain except at the surface where.
4. A time step calculation is performed, the time step employed in this work is designed so that it is not exceed the maximum step size permitted by stability. In this study the inviscid **CFL** conditions **[1]** is used which is given by the following relation: -

$$\Delta t)_{CFL} \le \left[\frac{|u|}{\Delta x} + \frac{|u|}{\Delta y} + \frac{|w|}{\Delta z} + a*\left[\frac{1}{(\Delta x)^2} + \frac{1}{(\Delta y)^2} + \frac{1}{(\Delta z)^2}\right]^{\frac{1}{2}}\right]^{-1} \qquad \ldots(15)$$

5. A changing of primitive variables to fluxes is occurred which causes to compute the values of flux vectors for all grid points at time step **(n).**
6. a forward predictor version of **MacCormack's** which is given by **[10] :-**

$$\overline{Q}_{i,j,k}^{n+1} = \overline{Q}_{i,j,k}^{n} - \frac{\Delta t}{\Delta x}\left[\overline{E}_{i+1,j,k}^{n+1} - \overline{E}_{i,j,k}^{n+1}\right] - \frac{\Delta t}{\Delta h}\left[\overline{F}_{i,j+1,k}^{n+1} - \overline{F}_{i,j,k}^{n+1}\right] - \frac{\Delta t}{\Delta z}\left[G_{i,j,k+1}^{n+1} - G_{i,j,k}^{n+1}\right] \qquad \ldots.(16)$$

is used inside the domain, where :-

n is the time level **(t)** and **n+1** is the time level **(t+dt).**

7. in order to make our numerical scheme accurate and stable, since we deal with high velocities (high Reynolds number) the following expression for explicit **artificial dissipation** is added to the predictor step, where $SQ_{i,j,k}^{n+1}$ is a fourth-order artificial viscosity term, defined by **[11]:-**

$$SQ_{i,j,k}^{n+1} = C_x \frac{\left|P_{i-1,j,k}^n - 2P_{i,j,k}^n + P_{i-1,j,k}^n\right|}{P_{i-1,j,k}^n + 2P_{i,j,k}^n + P_{i-1,j,k}^n} * \left[Q_1^-\right)_{i-1,j,k}^n - 2Q_1^-\right)_{i,j,k}^n + Q_1^-\right)_{i+1,j,k}^n \Big] +$$
$$C_h \frac{\left|P_{i,j-1,k}^n - 2P_{i,j,k}^n + P_{i,j+1,k}^n\right|}{P_{i,j-1,k}^n + 2P_{i,j,k}^n + P_{i,j+1,k}^n} * \left[Q_1^-\right)_{i,j-1,k}^n - 2Q_1^-\right)_{i,j,k}^n + Q_1^-\right)_{i,j+1,k}^n \Big]$$
$$+ C_z \frac{\left|P_{i,j,k-1}^n - 2P_{i,j,k}^n + P_{i,j,k+1}^n\right|}{P_{i,j,k-1}^n + 2P_{i,j,k}^n + P_{i,j,k+1}^n} * \left[Q_1^-\right)_{i,j,k-1}^n - 2Q_1^-\right)_{i,j,k}^n + Q_1^-\right)_{i,j,k+1}^n \Big] \quad \ldots(17)$$

The main advantage of artificial dissipation is to provide some mathematical dissipation analogous to the real viscous effects inside the shock wave.

8. A decoding is occurred which is used to produce our parameters from fluxes, also at this step, the contravarient velocity components which defined by :-

$$\begin{aligned} U &= x_x u + x_y u + x_z w \\ V &= h_x u + h_y u + h_z w \\ W &= z_x u + z_y u + z_z w \end{aligned} \quad \ldots(18)$$

are computed. The contravarient velocity components U, V and W represent velocity components which are perpendicular to planes of constant x , h and z

9. A corrector step is computed, where the value of fluxes (E ,F,G) are computed at each grid in the intermediate level (n+1) depending on the values of primitive variables from previous step, so the computations occurs inside the domain.
10. A backward corrector version of MacCormack's method which is given by [10] is then applied :-

$$Q_{i,j,k}^{n+1} = (1/2) * \left\{ \begin{array}{l} Q_{i,j,k}^n + \overline{Q}_{i,j,k}^{n+1} - \frac{\Delta t}{\Delta x}\left[\overline{E}_{i,j,k}^{n+1} - \overline{E}_{i,j-1,k}^{n+1}\right] \\ - \frac{\Delta t}{\Delta h}\left[\overline{F}_{i,j,k}^{n+1} - \overline{F}_{i,j-1,k}^{n+1}\right] - \frac{\Delta t}{\Delta z}\left[G_{i,j,k}^{n+1} - G_{i,j-1,k}^{n+1}\right] \end{array} \right\} \quad \ldots(19)$$

Which is used inside the domain, also a fourth-order artificial viscosity term [11] at corrector step is added to Eq.(19). This expression is given by:

$$SQ^{n+1})_{i,j,k} = C_x \frac{\left|P^{n+1}_{i+1,j,k} - 2P^{n+1}_{i,j,k} + P^{n+1}_{i-1,j,k}\right|}{\left[P^{n+1}_{i+1,j,k} - 2P^{n+1}_{i,j,k} + P^{n+1}_{i-1,j,k}\right]} * \left[\overline{Q}_1)^{n+1}_{i-1,j,k} - 2\overline{Q}_1)^{n+1}_{i,j,k} + \overline{Q}_1)^{n+1}_{i+1,j,k}\right] +$$

$$C_h \frac{\left|P^{n+1}_{i,j+1,k} - 2P^{n+1}_{i,j,k} + P^{n+1}_{i,j-1,k}\right|}{\left[P^{n+1}_{i,j+1,k} - 2P^{n+1}_{i,j,k} + P^{n+1}_{i,j-1,k}\right]} * \left[\overline{Q}_1)^{n+1}_{i,j-1,k} - 2\overline{Q}_1)^{n+1}_{i,j,k} + \overline{Q}_1)^{n+1}_{i,j+1,k}\right]$$

$$+ C_z \frac{\left|P^{n+1}_{i,j,k+1} - 2P^{n+1}_{i,j,k} + P^{n+1}_{i,j,k-1}\right|}{\left[P^{n+1}_{i,j,k+1} - 2P^{n+1}_{i,j,k} + P^{n+1}_{i,j,k-1}\right]} * \left[\overline{Q}_1)^{n+1}_{i,j,k-1} - 2\overline{Q}_1)^{n+1}_{i,j,k} + \overline{Q}_1)^{n+1}_{i,j,k+1}\right] \quad \ldots(20)$$

11. After a corrector step is completed, a decoding step began where our parameters such as (**u, v, w, P, T, e** and **M**) are computed.
12. Parameters are computed under different boundary conditions which can be explained as follows:-
   a. Up-stream boundary condition and at the edge of the body.
   b. Solid boundary condition.
   c. Down-stream boundary condition.
   d. Upper plane of symmetry.
   e. Plane of symmetry.
   f. far-field boundary condition.
13. The convergence of the solution is examined, knowing that the last flow field variable to be convergence is the density, therefore, the following convergence criterion was established at every point in the flow field from one time step to the next, where **[1]:**

$$\text{error} = \frac{r_{\text{old}} - r_{new}}{r_{old}} \le 1*10^{-8} \quad \ldots(21)$$

RESULTS AND DISCUSSION

Figure 1 shows a grid generation over a three-dimensional supersonic missile of different shapes in supersonic compressible external inviscid flow. The mesh points are produced by using an algebraic grid generation with (21 x 16 x 21) grid points. The explicit technique has required about (4000) time steps to achieve the converged solution (steady state solution). In the present work, the artificial viscosity is taken as (0.5), as shown in the figure.

Figures 2 and 3 show a Mach number and pressure contours for supersonic missile with conventional canard for free stream Mach number = 2.5. These figures show these parameters along the missile's body and on the missile's tail respectively for each value of free stream Mach number. The shock wave can be noticed clearly. The

flow pattern near the leading edge of supersonic missile, where the incoming supersonic flow undergoing a sudden change in flow direction resulting a continuous compression wave. The angle of the shock wave depends on the nose shape and free stream Mach number. The shock is observed to be detached from missile nose angle and flow behind the shock near the trailing edge of missile area becomes subsonic, also it's very important to refer that the clustering process is very necessary near the leading edge of supersonic missile in order to capture all the expected shock waves. This prediction gives a good agreement with the experimental results dealing with the same problem as indicated in [13]. It is very useful to note that the predicted shock wave by the numerical solution of the present work decelerate the flow speed from supersonic speed up stream of the shock wave to subsonic flow down- stream of the shock wave. Figure 3 indicate that the pressure distribution occurs at the region between the missile surface and the shock wave. Also, the pressure increases at the leading edge of the missile due to shock wave strength and is decreased gradually toward its free stream value. The higher pressure can be noticed at the edge of three-dimensional supersonic missile, due to shock wave effect.

Figure 4 explains a temperature contours over a three-dimensional conventional canard missile for free stream Mach number = 4.0. From this figure, the temperature values increases a head of shock wave and then decreased toward its free stream value away from the shock wave. This is agreeing with [14] and [15] also, the temperature values are increased dramatically near the leading edge of supersonic missile due to shock wave effects.

Figures 5 and 6 show the Mach number and temperature contours over a three-dimensional missile with no canard at free stream Mach number = 3.75. Again in these figures, the supersonic flow a head of the missile' nose cause a shock wave which can be noticed clearly. The Mach number at the outer domain of the flow field represents the free stream value which in this case equals to 3.75. Also, in this figure an important physical phenomena can be noticed where the higher intensity of the shock wave which comes from increasing of the Mach number which leads to reduce the distance between the predicted shock wave and the missile' nose. This prediction agrees with the same results predicted in [13], which noticed the same result during the analyzing another types of rockets. Also, the shock wave cone angle decreases with increasing the Mach number. Figure 7 explains the Mach number contours for a three-dimensional missile with long canard for free stream Mach number =3.75. The figure shows that the canard saves the wings of the missile from the shock wave. For this reason the wings in the missile studied with no canard is subjected to a higher temperature than the corresponding missile which use a canard. It is necessary to refer that this temperature leads to a dangerous thermal stresses.

CONCLUSIONS

The following conclusions can be drawn from the results of the present work:-

1. Geometry and supersonic missiles curvatures have an important effect on the flow field pattern; where in the supersonic flow the change in flow direction due to geometry induced a type of drag. This is called wave drag.

2. The time-marching solution which is used to deal with a three-dimensional supersonic missiles, which can be extended to deal with an axis-symmetry body such as aircraft
3. The software developed explains, that the convergence depends on the optimum values of the grid points, artificial viscosity and **CFL.**
4. The capturing the flow field parameters; a more mesh points are required near the surface of the supersonic missiles.
5. Since the mesh generation has been separated from explicit solver any mesh type can be used. The stability of the solution depends on the number of grid points and **CFL** condition. Clustering process is very necessary at the leading edge of the three-dimensional supersonic missiles in order to capture the expected shock wave.
6. The distance between the shock wave and a head of the missile's nose decreases with increasing the Mach number from (**2.5**) to (**4**). This behavior is due to higher intensity of the shock wave. The result of the present work explains that the number of iterations and the number of mesh points depending on Mach number. The result of the program indicate, that for the same Mach number, the increasing of mesh points, lead to increase of the number of iterations.

REFERENCES

[1]Hussein, Ahmed, K., "Numerical Simulation **o**f Flying Supersonic Body", PhD thesis, Al-Mustansiriya Univrsity, Baghdad, Iraq, 2006.

[2]Morgenstern, J.A., "Three-Dimensional Supersonic Flow Over a Spike – Nosed Body of Revolution", Journal of the Brazilian Society of Mechanical Sciences, Vol.24, No.4, 2002.

[3]Scalabrin, L.C., Azevedo, J.L., Teixeira, P.R. and Awruch, A.M., "Three-Dimensional Flow Simulations with the Finite Element Technique Over a Multi- Stage Rocket", Journal of the Brazilian Society of Mechanical Sciences and Engineering, Vol. XXVI, No.2**,** 2004, pp: 107-116.

[4]Wilcox, F., Birch, T. and Allen, J., "Force, Surface Pressure and Flow Field Measurements on a Slender Missile Configuration with Square Gross-Section at Supersonic Speeds", 22nd AIAA Applied Aerodynamics Conference**,** 2004, pp: 1-26.

[5]Blades, E. and Marcum, D., "Numerical Simulation of a Spinning Missile with Dithering Canards Using Unstructured Grids", Journal of Spacecraft and Rockets, Vol.41, No.2, 2004, pp: 248-256.

[6]Erickson, G., "Wind Tunnel Application of a Pressure – Sensitive Paint Technique to a Faceted Missile Model at Subsonic and Transonic Speeds", NASA/TM – 2004- 212991, 2004, pp: 1-40.

[7]Wu, P., Yong-Gang, M. and Chun, C., "The Research Analysis of Aerodynamic Numerical Simulation of Grid Fin", Journal of Zhejiang University SCIENCE, Vol. 6A, No.7, 2005, pp: 741-746.

[8]Cvitanovic, I., Virag, Z. and Krizmanic, S., "Analysis of Potential Flow around Wing-Body Configurations", 4th International Congress of Croatian Society of Mechanics (4th ICCSM), Bizovac, Croatia, 2005, pp: 1-11.

[9] DeSpirito, J., Vaughn, M.E. and Washington, W., "CFD Investigation of Canard-Controlled Missile with Planar and Grid Fins in Supersonic Flow", AIAA Atmospheric Flight Mechanics Conference and Exhibit, California, U.S.A, 2002, pp: 1-11.

[10]Hoffmann,A.K.,"Computational Fluid Dynamics for Enginering ", University of Texsas, 1989.

[11]Anderson, J.D. "Computational Fluid Dynamics**,** The Basic with Applications", McGraw-Hill Book Company, U.S.A., 1995.

[12]Wylie, C.R.," Advanced Engineering Mathematics "International Student Edition, MacGraw -Hill Book Company, U.S.A., 1966.

[13]Spearman, M. and Braswell, D., "Experimental and Theoretical Study of the Aerodynamic Characteristics of Some Generic Missile Concepts at Mach Numbers from 2.0 to 6.8 ", NASA Technical Memorandum 109110, 2002, pp: 1-30.

[14]Marsden, O., Bogey, C. and Bailly, C., "Higher-Order Curvilinear Simulations of Flows around Non-Cartesian Bodies", AIAA paper 2004-2813, 2004, pp: 1-15.

[15]Sorensen, N. "3D Background Aerodynamics Using CFD", Riso National Laboratory Publications, Roskilde, Denmark, 2002**,** pp: 1-18.

[16]Dietz ,W. , Wang ,L., Wenren ,Y., Caradonna, F. and Steinhoff, J. ,"The Development of a CFD-Based Model of Dynamic Stall", American Helicopter Society, 60 th Annual Forum, Baltimore, U.S.A., 2004, pp: 1-17.

List of Symbols:

Symbol	Description	Dimension
a	Speed of sound	m/s
CFL	Courant Fridrich Lewys stability condition	
C_x , C_ζ, C_η	Artificial viscosity coefficients in ξ, ζ and η directions respectively.	
e	Specific internal energy per unit mass	J/kg
E_t	Total energy per unit volume	J/m^3
E,F,G	Column vector in Cartesian coordinates	
$\overline{E}, \overline{F}, \overline{G}$	Column vector in body fitted coordinates	
J	Jacobian of coordinates transformation	
L	Length of the missile	m

M_∞	Free stream Mach number	
P_∞	Free stream pressure	N/m^2
Q	Flux vector	
$\overline{Q}$	Vector of conserved variable in body fitted coordinates	
Re	Reynold's number	
R	Universal gas constant	J/ kg. K
SQ_1	Artificial viscosity term	
t	Time	sec
T_∞	Free stream temperature	K
u	Velocity component in x-direction	m/sec
U	Contravariant velocity component in x -direction	m/sec
v	Velocity component in y-direction	m/sec
V	Contravariant velocity component in h -direction	m/sec
w	Velocity component in z-direction	m/sec
W	Contravariant velocity component in z -direction	m/sec
x, y, z	Cartesian coordinates	m

Greek Symbols

g	Ratio of specific heat capacities	
Δt	Time step	sec
r	Density	kg/m^3
a	Angle of attack	Deg.
d	Boundary layer thickness	m
$\Delta x, \Delta y, \Delta z$	Spatial steps in physical domain	
$\Delta z, \Delta h, \Delta x$	Spatial steps in computational domain	
z, h, x	Computational coordinates	

SUBSCRIPT

i, j ,k Node symbols indicates position in x ,y and z directions

∞ Conditions at free stream

o Stagnation (total) conditions

SUPERSCRIPT

n Time level t

n+1 Time level $(t + \Delta t)$

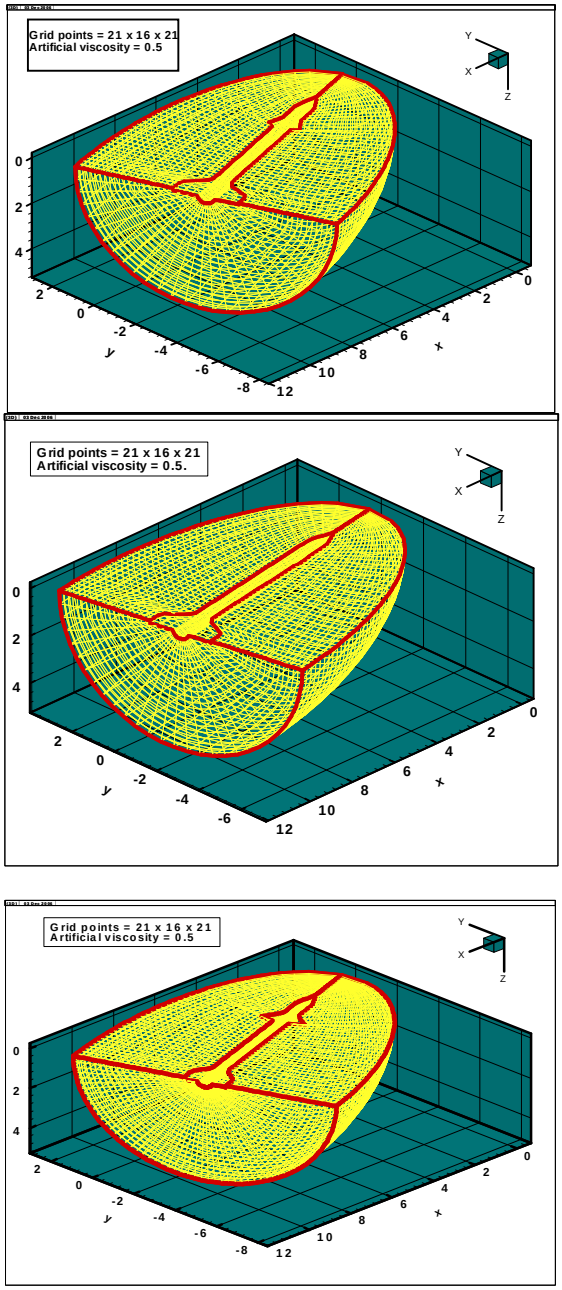

Figure (1) Algebraic grid generation over a three-dimensional supersonic missiles with mesh points (21 x 16 x 21).

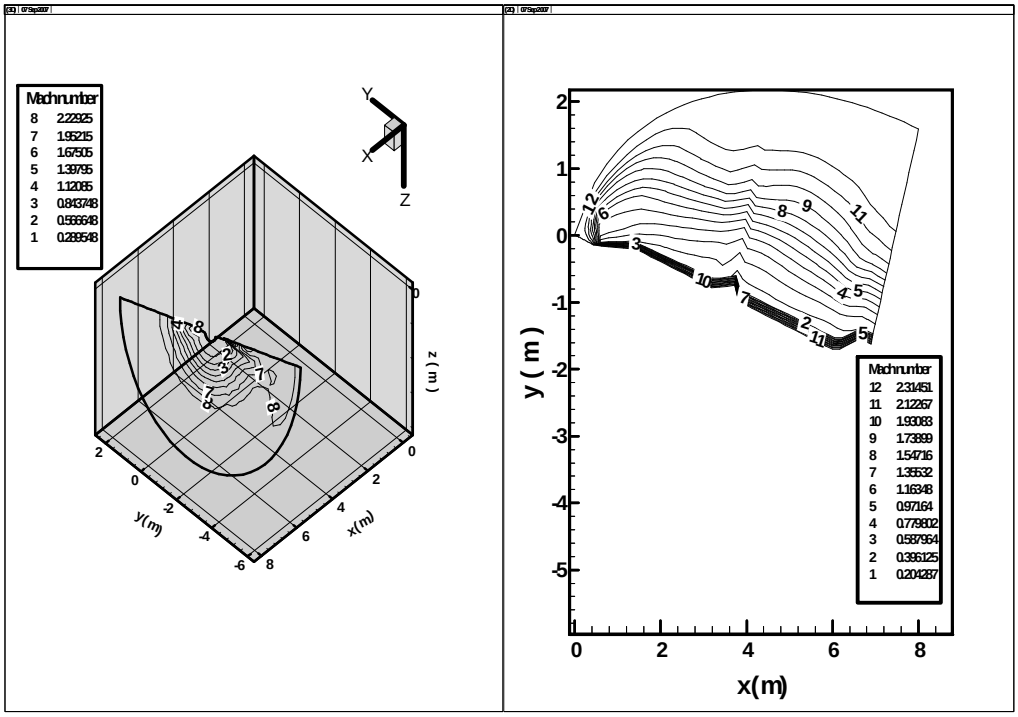

Figure (2) Mach number contours over a nose-canard-tail missile at free stream 2.5 Mach number.

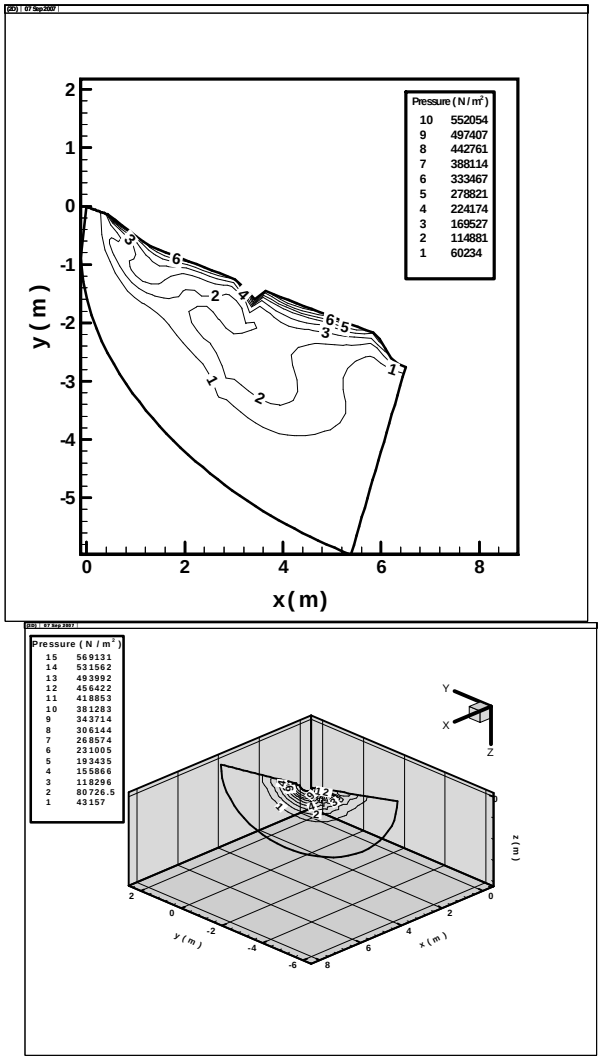

Figure (3) Pressure contours over a nose-canard-tail missile at free stream 2.5 Mach number.

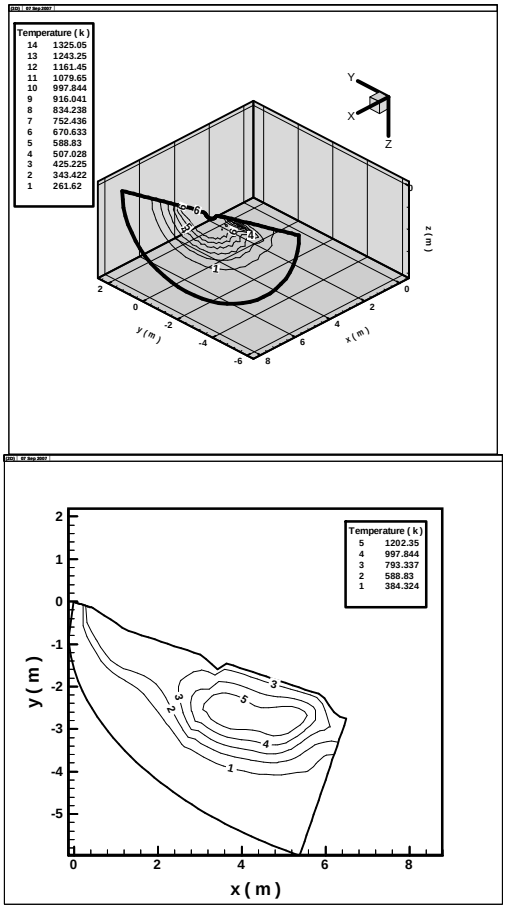

Figure (4) Temperature contours over a nose-canard-tail missile at free stream 2.5 Mach number.

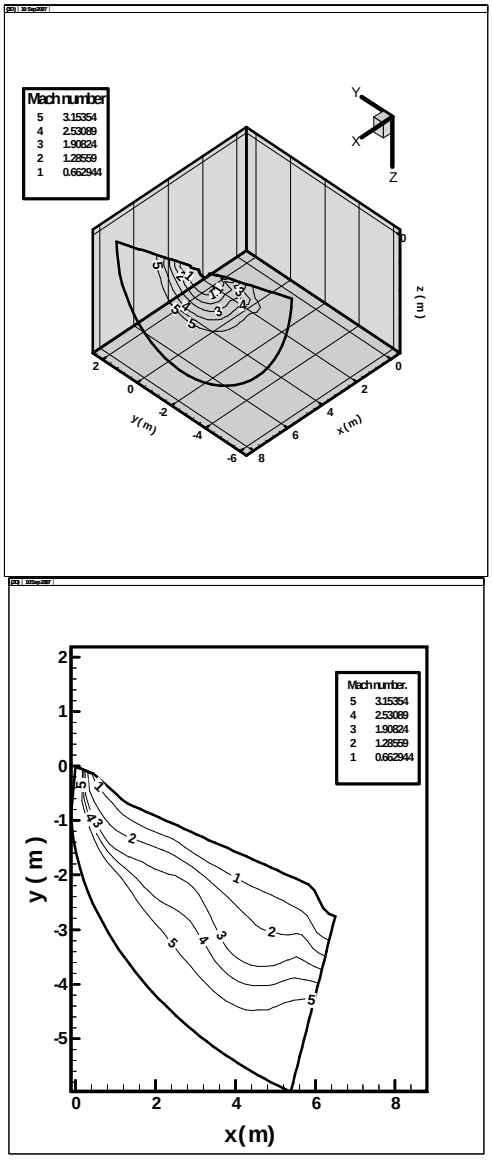

Figure (5) Mach number contours over missile with no canard at free stream 3.75 Mach number.

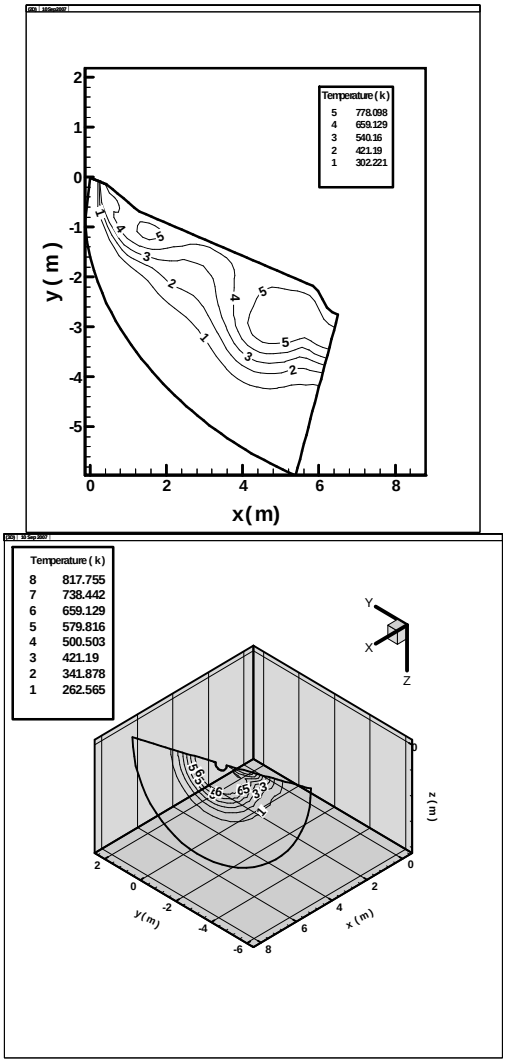

Figure (6) Temperature contours over a missile with no canard at free stream 3.75 Mach number.

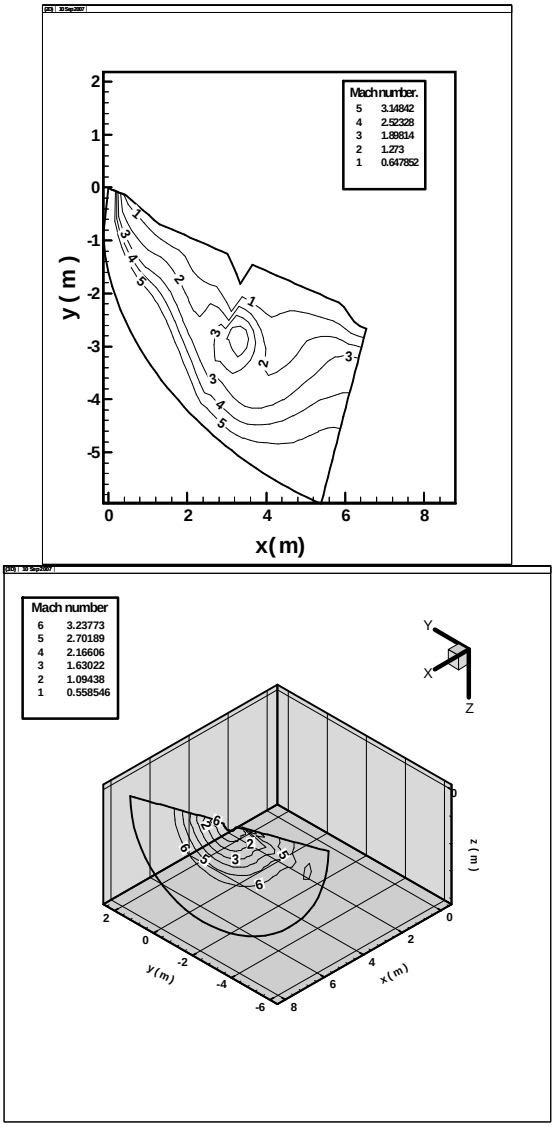

Figure (7) Mach number contours over a missile with long canard at free stream 3.75 Mach number.